
CHAPTER V

Study to Explore Host Guest Inclusion Complexes of Vitamin B₁ with CD Molecules for Enhancing Stability and Innovative Application in Biological System

Abstract: In this article the host-guest inclusion of thiamine hydrochloride (guest) within the hydrophobic cavity of α and β -cyclodextrin molecules (hosts) have been studied scientifically in the solid and solution phases respectively. Various modern spectroscopic techniques had been used to establish the outcome of this work. The UV-Vis study supported the 1:1 stoichiometry of the inclusion complexes and also used to evaluate the association constants along with thermodynamic parameters with high accuracy for the determination of the feasibility of this inclusion process. From the mass spectrometric study, 1:1 stoichiometry of the inclusion complexes had been confirmed in their solid state. Differential scanning calorimetric and infrared studies also supported this fact. ¹H-NMR and 2D ROESY spectroscopic analysis had given the mechanism of inclusion process, and the SEM study exposed their surface structures. Finally, the sustained oozing of the guest molecule from the hydrophobic cavity of the respective cyclodextrin molecules separately had been studied in the presence of human serum albumin in their aqueous buffer solutions with the help of fluorescence spectroscopic technique. This study has a truly intense effect to the stabilization of the respective guest molecule from the external hazardous, such as photolytic degradation, oxidation-reduction, thermal cleavage etc., and also predicts the releasing behavior of thiamine hydrochloride in the presence of human serum albumin without any chemical modification.

Keywords: Thiamine hydrochloride, Oligosaccharide, inclusion complexes, Human serum albumin, releasing behavior.

1. Introduction:

Oligosaccharides, specially cyclodextrins (CDs) regarding host-guest inclusion complexation have very significant importance in food industries[1],[2],[3] pharmaceuticals[4, 5]and consumer goods[6] due to their unique conical-shaped[7]cyclic structures. Cyclodextrins and their derivatives are commercially available and differ because of the presence of different glucopyranose residues. Cyclodextrins have their distinctive biphasic layers possessing hydrophilic outer and hydrophobic inner surfaces. The inner region allows incorporating hydrophobic surface of different guest or segment(s) of guest molecules into the cavity of a suitable and stable geometrical sized CDs through various kinds of non-covalent interactions[8]·[9]. Herein, α and β -cyclodextrins bearing 6 and 7 glucopyranose units, respectively, have taken as host molecules. Due to high inclusion efficiency, fitting cavity dimensions, low price, and negligible toxicity[10, 11].The CDs have found widespread application in pharmaceuticals[12], food industries[13], cosmetics[14], tissue engineering[15], biomedical devices.[12, 16]Inclusion complexation within the non-polar cavity of CDs (**Figure 1**) is employed for protecting the hydrophobic part of different bioactive molecules[17],enzymes[18, 19], drugs[20], volatile organic compounds, flavors[21], essential oils [22, 23], taxols [24], flavonoids [25], vitamins[26], and etc. to extend their light, air and thermal stability, enhancement of water solubility, bioavailability and shielding side effects.

The B vitamins and their derivatives are a class of water-soluble vitamins and naturally found in food substances. These have significant role in cell metabolism[27]. They have major importance for food processing and biological activities such as transferring the alkyl group, fitting carbon dioxide, decarboxylation and transamination of amino acids, lipids and sugars[28-31]. Fruit juices are one of the main sources of vitamins and the quality of fruit juices in industry is maintained by different techniques including pasteurization, which led to the degradation of vitamins along with other valuable food nutrients. Day to day Consumer's realization about food nutritional value is throwing a challenge to the companies for healthier foods without any change in their chemical properties[32, 33]. Among all the B vitamins and their derivatives, one of the

most common is thiamine (vitamin B₁) chloro hydrochloride (THC, **Figure 1**), which is usually used as a component of single vitamin B complex and multivitamin preparations, food supplement, antioxidant, prooxidant, pharmaceutical industries and biological fluids. THC is used to treat in appetite and dermatophytosis. Moreover, it is also helpful to metabolize in human body.[34].[32, 35-37]Due to the lack of thiamine hydrochloride, neurotransmission in human body can be affected. Deficiency of THC leads to the occurrence of various malfunctions inside the human body such as beriberi, Wernicke-Korsakoff syndrome, confabulation and an irreversible dementia; even extreme deficiency may lead to heart failure and death[38].[39],[40]. Thus thiamine hydrochloride is extensively used in human body; moreover, it can be utilized as feed in agriculture and synthetic intermediates in industry[41].But THC is very sensitive to light and high temperature processing and also has tend to get oxidize easily in the presence of oxygen which limits their applications to a great extent in different fields. Chemical degradation is very common with vitamin B1 and the main route of the degradation is its reduction which is caused in the presence of food preservatives such as sodium metabisulfite, with very low concentrations (~1 mmol/L). Moreover, it can degrade by some of cell surface enzymes and plant thiamine antagonists[31, 33, 42].

Based on molecular recognition, inclusion of THC into CDs offers potential advantages in delivery without changing its chemical characteristics. In order to overcome all of these above mentioned foremost problems, we have attempted inclusion of THC within the hydrophobic cavity of α - and β -CD to improve stability and natural characteristics involving preservation for a long existence of time. Several studies have been done to find out the stability of THC within the cavity of CDs against the aforementioned adverse effect.

Human serum albumin (HSA) is one of the most abundant and popular protein in blood-plasma having 585 amino acid sequences. HSA consists of long chain polypeptides. It has tertiary structure consisting of three domains named I, II and III respectively. HSA has only one tryptophan residue (Trp-214) which is located in the sub-domain IIA. HSA plays a very important role for the maintenance of life systems.[43].[44-46]According to the two scientists Helms et al. and EI-Kemary et.al., serum proteins can take up many

conformations from the range of close compact to relaxed form. In recent years, there is an ongoing interest and a large field to investigate of plasma proteins with smaller molecules such as drugs, vitamins, hormones and other different kinds of bioactive molecules. The metabolism, distribution, free concentration can change significantly due to binding of HSA[44, 47],[48],[49],[50],[51]. In the other side, high intake of THC causes several effects such as developing cataracts, kidney disease and dysmenorrheal [52-54]. So, regular dischargement of THC at the targeted site for long term effectively is very important. In this work to get an idea about the regular releasing behavior of THC from the CDs cavity separately in the human body, HSA has taken which will help to formulate THC in pharmaceuticals and food industries.

In this novel work, the inclusion of THC has been aimed within the cavity of α and β -CD separately in both solution and solid states to explore their formation of inclusion complex (IC) for enhancing the stability of THC. Regular release without any chemical alteration of THC in the presence of HSA from the cavity of α and β -CD separately have been monitored with the help of fluorescence spectroscopy. Formation of inclusion complexes have been well characterized by various reliable techniques like 2D ROESY and ^1H NMR, IR, UV-Visible spectroscopy, Fluorescence spectroscopy, DSC, ESI-MS, SEM study has been done to get an idea about the surface nature of the corresponding two inclusion complexes. Association parameters, thermodynamic parameters, and stoichiometry have been evaluated to get a clear and quantitative idea about the formation of these ICs.

Hence, this present work mainly approaches towards the stability and regular release of THC inside the body and helps to execute the proposed utilization in the field of food chemistry and pharmaceutical science.

2. EXPERIMENTAL SECTION

2.1. Materials:

Thiamine hydrochloride having purity $\geq 98.0\%$ was purchased from TOKYO CHEMICAL INDUSTRY CO., LTD while human serum albumin, α - and β -cyclodextrins of high purity

grade $\geq 97.0\%$ and $\geq 98.0\%$ respectively were purchased from Sigma-Aldrich, Germany. All of these samples were kept in the refrigerator as received and used during the following experiments without further any alteration.

2.2. Apparatus:

UV-Visible spectra were recorded with the help of Agilent 8453 UV-Visible Spectrophotometer with an uncertainty of wavelength accuracy of ± 0.5 nm and an automated digital thermostat was used to control the temperature of the cell during performing the experiments.

$^1\text{H-NMR}$ and 2D ROESY spectra were recorded in D_2O solvent at 400 MHz in Bruker Avance instrument at 298.15 K. All the signals are shown in terms of δ values (in ppm) by using residual protonated solvent signal (HDO: δ 4.79 ppm) as internal standard and all the data are represented in the form of chemical shift (δ) values.

The DSC thermograms of the samples were recorded with the help of Perkin-Elmer DSC-6 differential scanning calorimeter at the heating rates of $10^\circ\text{C min}^{-1}$. The thermogram was taken by heating 1 mg of samples in aluminum crimped pans under nitrogen gas flow within the temperature range $30\text{--}300^\circ\text{C}$.

ESI-MS analyses were performed by Q-TOF high resolution are shown with positive mode electro-spray ionization taking the methanol solution of the solid ICs.

According to KBr disk method, FTIR spectra were recorded on a Perkin-Elmer spectrometer within $4000\text{--}400\text{ cm}^{-1}$ scanning range at room temperature. All KBr disks were made in 1:100 ratios of sample to KBr and during the experimental studies humidity was at 45%.

SEM images had been recorded with the help of JEOL JSM IT 100 Scanning Electron Microscope (SEM) to determine surface morphology. Samples were prepared on a small

piece of double adhesive carbon-coated tape attached to brass stubs and then a coating of ultra-thin layer of gold ions was put in a gold-ionization chamber. SEM images were recorded at various resolutions.

Fluorescence spectra were recorded with the help of Bench top spectrofluorimeter from photon technologies International (Quantamaster-40, USA) at room temperature. Data were recorded by taking solutions into Hellma quartz cuvette having optical path length 1.0 cm while excitation and emission slit widths fixed at 5.0 nm and 5.0 nm, respectively.

2.3. Procedure:

Solubility of all the required compounds was specifically checked in triply distilled and de-ionized water. Mettler Toledo AG-285 having uncertainty ± 0.0003 g was used to prepare all the solutions of THC, HSA, α - and β -CD by mass at room temperature. All the stock solutions were prepared by mass dilution and freshly prepared solutions were used during each experiment in phosphate buffer aqueous solution of pH 7.4. Sufficient precautions had been taken during measuring weights, preparing solutions and performing all the respective experiments. Two solid ICs, THC+ α -CD and THC + β -CD had been prepared in 1:1 molar ratio of THC and CD. 1.0 mM of α - and β -CD were each separately mixed with water and stirred for 4 hours. After that the aqueous solution of 1.0 mM of THC was added drop wise to the respective solutions of CD and left for stirring near about 36 hours at 50-55 °C to prepare the corresponding two ICs. Just after filtration of the hot solutions, it is allowed to cool down to 5°C and kept for 12 hours without any disturbing. The obtained suspension was then filtered and washed with ethanol and dried in air to get white polycrystalline powder.

3. Result and Discussion

3.1. Job plot: Stoichiometry of the host-guest inclusion complex

The well-established Job's method, usually known as continuous variation method is used to find out the stoichiometry of host-guest inclusion complex[55]. For this UV-Visible study, a set of solutions of THC had been taken along with host α and β -CD separately varying mole fractions within the range of 0-1 (**Table S1-S4**) in aqueous

solution and experiment was done at 298.15 K. The THC has absorbance with respect to two λ_{max} 's regarding $\Pi-\Pi^*$ transitions, $\lambda_{\text{max}} = 236$ nm for pyrimidine ring and = 263 nm for thiazole ring. Hence, the absorbance of THC had been taken at $\lambda_{\text{max}} = 236$ nm and 263 nm respectively (**Figure 2**) for the set of prepared solutions. $\Delta A \times R$ vs. R were plotted (**Figure 3**) of THC+ α -CD and THC + β -CD for the graph of Job's plot separately where, ΔA is the difference in absorbance of THC without and with CDs and "R" refers to the mole fraction of THC, i.e. $[\text{THC}] / ([\text{THC}] + [\text{CD}])$. The Y-axis in the Job's plot represents physical property ($\Delta A \times R$), that functions as a proxy for the concentration of inclusion complex. From the value of R at the maxima of the plots, the stoichiometry of inclusion complex can be obtained for example if the value of R is 0.33, 0.5 or 0.66 then the stoichiometry of host-guest inclusion complex is 1:2, 1:1 or 2:1 respectively[56]. In this experimental study the value of R had been obtained ~ 0.5 from the four plots at $\lambda_{\text{max}} = 236$ and 263 nm for α and β -CD correspondingly which clearly indicates the host-guest inclusion stoichiometry 1:1 for both the cases [57](**Figure 3**) that means both the pyrimidine and thiazole ring form 1:1 inclusion complexes with the respective CDs separately. So, it can be concluded that there is a high probability of formation of a dynamic equilibrium among the pyrimidine and thiazole part of THC with the respective CDs separately in the aqueous solution phase.

3.2. Ultraviolet spectroscopy for the determination of association constants of the ICs:

The non-covalent binding capability of the guest molecule within the cavity of host supra-molecules and the binding strength of the respective inclusion complexes had been explored by the evaluated association constants (K_a) of the ICs in the solution state with the help of UV-Visible spectroscopy[20]. The molar extinction co-efficient (ϵ) of the chromophore of THC was changed on the basis of the solvent polarity as it was changing its environment from polar aqueous medium to apolar cavity of CDs via non-covalent interactions to form host-guest inclusion complexes[58]. For the determination of K_a , the change in absorbance (ΔA) of THC at $\lambda_{\text{max}} = 236$ and 263 nm for pyrimidine ring and thiazole ring respectively was measured with gradual increasing the concentrations of α - and β -CD separately by varying temperature within the range of 298.15 to 308.15 K

(Table S5-S8). The double reciprocal plots (**Figure S1-S2**) were drawn with the help of Benesi-Hildebrand method[59],[60],[61]for 1:1 host - guest complexation and the corresponding equation is given as follows

$$\frac{1}{\Delta A} = \frac{1}{\Delta \varepsilon [THC] K_a} \frac{1}{[CD]} + \frac{1}{\Delta \varepsilon [THC]} \quad (1)$$

Where ΔA is the change in absorbance of THC (at $\lambda_{max} = 236$ and 263nm) and $\Delta \varepsilon$ is the change in molar extinction co-efficient of THC from polar environment to apolar environment. The resulting plots are straight line and the K_a for the ICs are evaluated from the intercept to slope of the straight line of the double reciprocal plot (**Table 1**).

K_a 's for the respective IC's were also determined with the help of non-linear programmed by the UV-visible study owing to the encapsulation of THC within the hydrophobic cavity of α -CD and β -CD separately. As a result of formation of 1:1 IC in the solution phase, there should be an equilibrium established between host and guest molecules[58, 62, 63].



The association constant (K_a^r) for the above equation can be expressed as follows

$$K_a^r = \frac{[IC]}{[THC]_f [CD]_f} \quad (3)$$

Where $[IC]$, $[THC]_f$ and $[CD]_f$ refer the equilibrium concentrations of IC, free THC and free CD respectively for the above mentioned reaction equation. According to the binding isotherm, the (K_a^r) for the for the formation of ICs can be written in terms of their absorbance as follows

$$[CD]_f = [CD]_x - \frac{[THC]_x (A_{obs} - A_0)}{(A - A_{obs})} \quad (4)$$

Here, A_0 is the initial absorbance for THC molecule, A_{obs} is the absorbance of the THC in the time of ongoing addition of CDs and A denotes the final concentration of THC molecules. $[THC]_x$ and $[CD]_x$ are the concentrations of cyclodextrin and THC molecules respectively. The obtained (K_a^r) values the respective ICs at both λ_{max} values are listed in the **(Table 1)** with the help of non-linear programmed.

The association constants of the IC's define the binding ability of the guest into the host as well as their stability as IC. The greater values of the association constants for IC's describes the greatness of their stability. From the Table 1, it is clear pyrimidine part of the THC binds more strongly than that of the thiazole part of THC. The IC's formed with β -CD were found more stable than that of the IC's formed with α -CD. With increasing temperature, the thermal stability of IC's decreases as the encapsulation of the guest into host cavity leads to the decrease in enthalpy **(Table 2)**.

3.3 UV-Visible spectroscopy, Non-linear program based mathematical calculation to determine the thermodynamic parameters:

Thermodynamic parameters were calculated basing on the association constants(K_a, K_a^r) obtained from a variety of isotherms by the above mentioned linear and non-linear methods with the help of van't Hoff equation[20, 64, 65]**(Figure S3-S4, Table S9-S10 and Figure S5-S6, Table S11-S12)**.

$$\ln K_a = -\frac{\Delta H^0}{RT} + \frac{\Delta S^0}{R} \quad (5)$$

$$\Delta G^0 = \Delta H^0 - T\Delta S^0 \quad (6)$$

where ΔH^0 , ΔS^0 , R and T carry their usual meanings. The calculating value of ΔH^0 and ΔS^0 for the formation of ICs were suggesting that the entire inclusion complex formation process in the solution phase are exothermic and entropy restricted means the process is unfavorable in terms entropy **(Table 2)**. From these results it can be concluded that the entire inclusion complex formation process in solution phase is thermodynamically

spontaneous but entropically unfavorable as molecular recognition takes place and is highly diminished by the greater value of change in enthalpy ($\Delta H^0, \Delta H^{00}$) hence makes the overall process thermodynamically favorable. Thus the Gibbs free energy ΔG^0 becomes negative directing spontaneity in the formation of the ICs

3.4 ^1H NMR and 2D ROESY NMR spectra analysis of solid inclusion complexes

In order to explain the mechanism of the inclusion complexation of THC with the respective cyclodextrin molecules, ^1H -NMR and 2D-ROESY spectra were recorded. The ^1H -NMR spectra and the chemical shift (δ) values of THC, α -CD, β -CD and their inclusion complexes are shown in the **Figure S7-S11** and in **Table S13** respectively. As a result of mutual shielding through space among the interacting protons of THC with that of the cyclodextrin molecules, there is a change in their NMR spectra in their corresponding inclusion complexes. Here, change of the chemical shift values of protons of cyclodextrin supramolecules occurs through diamagnetic shielding mainly by the aromatic segments of THC molecule. From the structure of CD (**Figure 1**), it can be seen that H3 protons and H5 protons are situated at the wider and narrower rim sides respectively while the rest of protons are at the exterior area of the CD conical shaped molecule. From the **Figure S7-S11** of NMR spectra it is clearly seen that there is a upfield shift of H3 and H5 protons of α and β -CD correspondingly which confirms the formation of inclusion complexes with the THC molecule.

To get the clear idea about the mode of interactions of the protons of THC molecule with that of the CD molecules in their inclusion complexes 2D ROESY NMR had been performed and the spectra are shown in **Figure 4 & 5**. There are some diagonal and off-diagonal peaks are observed in the spectra in ROESY NMR for the THC-CD complexes if protons are situated within 0.4 nm in space. Off-diagonal peaks are due to the inter cross correlation of the protons of THC with the interior protons i.e. H3 and H5 of CD molecules. In the **Figure 4 & 5**, there are three off-diagonal peaks are observed due to the inter molecular dipolar cross correlation between H-6 proton of THC with the H3 and H5 of α and β -CD while H-1 and H-7 of THC with H3 and H5 of α and β -CD molecule

respectively suggesting that the pyrimidine part of THC strongly interacts with the interior protons of CD molecules and resides inside the CD cavity but there is a weak interaction between the thiazole moiety of THC with the CDs probably that positive charge on the N atom of thiazole moiety resists it to stay within CD hydrophobic cavity. As there is no such significant peaks with the H6 protons of CD with that of the THC molecule, it can be concluded that the inclusion occurs through wider rim side (**Figure 6**) for both α and β -CD otherwise some changes will be observed as H6 protons reside near narrower side of the rim.

3.5 Differential scanning calorimetric (DSC) study

The thermal characterization of the inclusion complexes had been done with the help of DSC technique[66]. Each pure compound has its own characteristic boiling, melting or sublimation point which frequently disappears or shifts to the different temperature due to the formation of inclusion complexes[67],[68],[69].The DSC thermograms of THC and its ICs are shown in the **Figure 7**. The DSC thermogram of THC showed a sharp endothermic peak at 252.28 °C corresponds to its melting point. In the ICs a characteristic peak with large shifting in comparison with the THC to the different temperatures were observed. Initially endothermic peaks at 67.81 °C and 140.50 °C for IC-1 could be attributed to the loss of water due the evaporation. Similarly, endothermic peak at 62.67 °C for IC-2 is due to the loss of water molecules owe to the evaporation. Both the peak at 228.81°C for IC-1 and at 226.17°C for IC-2 indicate the loss of crystalline nature of THC molecule and also suggesting that there is a strong interaction of THC molecule with β -CD compare to α -CD.

3.6 ESI-mass spectrometric analysis of inclusion complexes

The ICs of THC with α -CD and β -CD separately were further investigated in their solid state with the help of ESI-mass spectrometry by dissolving in methanol. The observed spectra are shown in **Figure 8**. The peaks at m/z 1238.44 and 1260.42 correspond to the $[\text{THC} + \alpha\text{-CD} + \text{H}]^+$ and $[\text{THC} + \alpha\text{-CD} + \text{Na}]^+$ respectively and the peaks at m/z 1400.49 and 1422.47 correspond to $[\text{THC} + \beta\text{-CD} + \text{H}]^+$ and $[\text{THC} + \beta\text{-CD} + \text{Na}]^+$ respectively. From all of this values, it can be concluded that the ICs of THC with α -CD and β -CD separately have

been formed in the solid state and the obtained stoichiometric ratio is 1:1 for the host to guest molecule[70].

3.7 FT-IR spectra of solid inclusion complexes

The formation of inclusion complexes are also well explained with the help of infrared spectroscopic technique[71], [72], [73]. KBr disk method had been used to get the IR spectra of the pure THC, α -CD, β -CD and their respective IC's which are shown in the **Figure 9**. The noteworthy signals which are shifted sufficiently have been listed in the **Table S14**.

For IC-1 means (α -CD+THC) system, the following spectral changes are obtained due the host-guest interactions. (i) The broad signal at 3436.04cm^{-1} of THC generally found due to the merging of the two signals respective to $-\text{NH}_2$ and $-\text{OH}$ groups together and this peak is found to shift at 3420.09 cm^{-1} in IC-1 while 3410.09cm^{-1} is observed for $-\text{OH}$ groups in α -CD. (ii) The signal of 2361.26 cm^{-1} for ($\text{C}^{\text{sp}^3}\text{H}_2$) bending of THC is shifted to 2365.21 cm^{-1} in the complex. (iii) The peak at 1636.35 cm^{-1} for N-H (NH_2) bending of THC is obtained at 1632.02 cm^{-1} while complexed with α -CD. (iv) The peaks from 519.08 cm^{-1} to 1380.15 cm^{-1} of THC are almost completely masked in its complex with α -CD.

For IC-2 means (β -CD+THC) system, the following changes in their spectra are observed owe to the various non-covalent interactions of THC with β -CD. (i) The signal at 3424.05 cm^{-1} for $-\text{OH}$ stretching of β -CD is changed to 3401.23cm^{-1} in IC-2. (ii) The peak at 2361.26 cm^{-1} for ($\text{C}^{\text{sp}^3}\text{H}_2$) bending of THC is shifted to 2363.29 in its complex with β -CD. (iii) The peak at 1636.35 cm^{-1} for N-H (NH_2) bending of THC is now changed to 1632.27 cm^{-1} . (iv) The signals in the range of 519.08 cm^{-1} to 1380.15 cm^{-1} are also just as IC-1 masked significantly in IC-2.

Thus, from the above discussions along with the **Figure 9** and **Table S14**, it was seen that, there is no significant appearance of new signals which clearly indicate the absence of formation new chemical bonds between THC and CDs. So, it can be clearly said that the slight shifting of some significant IR signals that may signify hydrophobic-

hydrophobic as well as non-covalent interaction of thiazole and pyrimidine ring of THC with CDs causing random weakening and strengthening of the interacting bonds while formation of IC's.

3.8 Scanning Electron microscopic (SEM) study to exhibit the surface structures:

Scanning electron microscopy (SEM) is a well-established technique to analyze the surface morphology and the particle size of the solid substances [9, 59, 74]. The surface morphology of the pure guest THC, pure hosts α and β -CD separately, their respective ICs and their corresponding physical mixtures have been shown in the **Figure 10 & 11**. From the SEM images, it is clear that the surface morphology of the ICs is totally different from their raw materials which indicates the formation of new morphology probably indicating the formation of host-guest inclusion complexes as evident from the above mentioned different experimental studies.

3.9. Steady-state fluorescence: Association constants from Modified Benesi-Hildebrand equation and association constants.

The association constants of THC molecule with and without the presence of CD molecule had been derived from the modified Benesi-Hildebrand equation by using spectrofluorimetric method [75], [76], [77].

$$\frac{1}{I - I_0} = \frac{1}{[I' - I_0]K_a^\phi} \frac{1}{[THC]} + \frac{1}{I' - I_0} \quad (7)$$

Where, I and I_0 represents the fluorescence intensities of HSA in the presence and absence of the THC respectively, I' are the intensities of the HSA while all the guest molecules for a particular system are complexed with THC. $[THC]$ represents the concentration of the Thiamine hydrochloride.

From the above discussions it is clear that there is a formation of 1:1 inclusion complex of THC with CDs. All the fluorescence spectra are taken by exciting the HSA at λ_{\max} 280 nm by keeping constant the volume and concentration of HSA and CDs in the

respective aqueous solution mixtures while the concentration of THC was varied. The whole experiment was done at phosphate buffer aqueous solutions by maintaining pH 7.4 at 298.15 K. From the plots (**Figure S12**) drawn by using the above mentioned equation, association constants are evaluated which are shown in **Table S15-S17**, suggesting the stability of the newly formed complexes in the solution phase at room temperature. The Gibbs free energy value (**Table 3**) suggesting the spontaneity of the whole complexation processes.

3.10. Binding interaction of the THC molecule in the presence of human serum albumin with and without CDs: The process of dischargement of guest from the cavity of CDs

Fluorescence spectroscopy is a very useful and highly sensitive technique to inspect the change in the microenvironment around the fluorophore depending on the binding with quencher[78],[79].

Thus from this study lots of different kind of useful information can be obtained with respect to the binding mechanism[47, 48, 80]. The release of THC from the inclusion complexes was determined with the help of fluorescence emission spectroscopy by observing the binding interaction of HSA with THC in the presence and absence of CDs in aqueous medium. The intrinsic fluorescence of HSA is due to Trp 214 (hydrophobic moiety) alone having λ_{\max} of 280 nm.

For all the set of solutions, excitation had been done at 280 nm to investigate the shift of λ_{\max} and the intensity of the HSA molecule with and without the presence of CD molecules, the corresponding spectra was shown in the **Figure 12**. From these figures, hypochromic shift i.e. a regular decrease in the intensity of the spectra with increasing the concentrations of THC separately in the aqueous buffered solutions of HSA along with respective CDs, was clearly observed probably as a result of strong non-covalent interactions of fluorophore moiety of HSA molecule with the THC molecule. The binding constants of THC:HSA in the presence of CD molecule are 3.03×10^3 and $2.49 \times 10^3 \text{ M}^{-1}$ for α and β -CD respectively, where $4.21 \times 10^3 \text{ M}^{-1}$ for THC: HSA without CDs suggesting there

is a less association of THC with HSA molecule in the presence of CDs as inclusion of THC with CDs decreases the strength of their binding by blocking the non-covalent interactions existing between them. So, HSA strongly competes with CDs to bind THC and in this way it helps in effective delivery of vitamins. Accordingly, it enhances the availability of free THC in blood plasma resulting effective therapeutic effect at the target site. This study also proves the formation of inclusion complexes of THC with both α and β -CD respectively in solution phase.

Hence from this experimental study we can conclude that there is a regularity in the oozing of the guest molecule from the cavity of CDs into the aqueous solution in the presence of HSA molecule.

4. Conclusion

1:1 host-guest inclusion complexes of THC within the cavity of α and β -CD are well established by the various techniques in solution phase as well as in the solid state. The entire inclusion process is thermodynamically feasible process as obtained from the calculated thermodynamic parameters and evaluated association constants reveal the stability of the formation of ICs. Molecular recognition due to the dimensional suitability is the major stabilizing factor. The positive entropy factor is also responsible for the formation of ICs via non-covalent interactions such as hydrogen bonding and other hydrophobic interactions as more number of water molecules compare to that of THC molecule are released from the cavity of the CDs for making the free suitable space for the incoming THC molecule. Formation of inclusion complexes enhances the photochemical stability of THC, protect it from thermal degradation and retain its property without any kind of chemical transformation. Moreover, the regulatory dischargement of THC molecule at pH 7.4 from the hydrophobic cavity to the polar aqueous media has been clearly explained in the presence of HSA molecule. So, there is a strong probability to show similar kind of binding behavior of THC with HSA in the human body and successfully will be delivered to the targeted area as per required amount of it. Hence the study for the formation of inclusion complex and the regulatory dischargement of THC from the hydrophobic cavity of CDs into the aqueous solution approach a novel way for the versatile uses and formulation in food, medicinal and

pharmaceutical industries without any chemical modification. In conclusion, this article demands far reaching effects by dint of innovative applications in pharmaceutical science.

Acknowledgement

Prof. M. N. Roy would like to acknowledge UGC, New Delhi, Government of India, for being awarded One Time Grant under Basic Scientific Research via the grant-in-Aid no. F.4-10/2010 (BSR). BR is thankful to the "State Fellowship" bearing reference No. 1743/R-2017 dated 18.04.2017. Mr. Goutam Sarkar, The H.O.D., USIC, University of North Bengal, Darjeeling is also highly acknowledged for executing SEM associated with this paper.

Disclosure of interest

The authors declare no conflicts of interest.

TABLES

Table 1: Association Constants derived from Benesi-Hildebrand method (K_a) and also from the Nonlinear Program (K_a^r) using UV-Visible spectroscopic data at 236 to 263 nm in the temperature range 298.15 to 308 K.

Host	λ_{\max} (nm)	Temperature (K ^o)	K_a ($\times 10^3$)	K_a^r ($\times 10^3$)
α -CD	236	298.15	1.28	1.30
		303.15	1.12	1.10
		308.15	0.86	0.87
	263	298.15	1.12	1.22
		303.15	0.85	0.81
		308.15	0.62	0.64
β -CD	236	298.15	1.90	2.10
		303.15	1.62	1.52
		308.15	1.33	1.23
	263	298.15	1.67	1.47
		303.15	1.50	1.20

		308.15	1.13	0.93
--	--	--------	------	------

^aStandard uncertainty in temperature, u, are u(T) = ± 0.01 K

Table 2: Thermodynamic parameters (ΔH^0 , ΔS^0 , ΔG^0) and ($\Delta H^{0\tau}$, $\Delta S^{0\tau}$, $\Delta G^{0\tau}$) calculated, using the association constants (K_a , K_a^τ) obtained from Benesi-Hildebrand method, Nonlinear Program for λ_{\max} =236 nm and 263 nm.

Inclusion Complexes (ICs)	λ_{\max} (nm)	Application of (K_a) to Van't Hoff equation		Application of (K_a^τ) to Van't Hoff equation	
		ΔH^0 (KJ mol ⁻¹)	ΔS^0 (J mol ⁻¹ K ⁻¹)	$\Delta H^{0\tau}$ (KJ mol ⁻¹)	$\Delta S^{0\tau}$ (J mol ⁻¹ K ⁻¹)
THC + α -CD	236	ΔH^0 (KJ mol ⁻¹)	-30.07	$\Delta H^{0\tau}$ (KJ mol ⁻¹)	-30.32
		ΔS^0 (J mol ⁻¹ K ⁻¹)	-41.20	$\Delta S^{0\tau}$ (J mol ⁻¹ K ⁻¹)	-41.98
		ΔG^0 (KJ mol ⁻¹)	-17.79	$\Delta G^{0\tau}$ (KJ mol ⁻¹)	-17.80
	263	ΔH^0 (KJ mol ⁻¹)	-44.77	$\Delta H^{0\tau}$ (KJ mol ⁻¹)	-48.97
		ΔS^0 (J mol ⁻¹ K ⁻¹)	-91.69	$\Delta S^{0\tau}$ (J mol ⁻¹ K ⁻¹)	-105.35
		ΔG^0 (KJ mol ⁻¹)	-17.43	$\Delta G^{0\tau}$ (KJ mol ⁻¹)	-17.56
THC + β -CD	236	ΔH^0 (KJ mol ⁻¹)	-27.11	$\Delta H^{0\tau}$ (KJ mol ⁻¹)	-40.81
		ΔS^0 (J mol ⁻¹ K ⁻¹)	-28.11	$\Delta S^{0\tau}$ (J mol ⁻¹ K ⁻¹)	-73.42
		ΔG^0 (KJ mol ⁻¹)	-18.73	$\Delta G^{0\tau}$ (KJ mol ⁻¹)	-18.92
	263	ΔH^0 (KJ mol ⁻¹)	-29.59	$\Delta H^{0\tau}$ (KJ mol ⁻¹)	-29.59
		ΔS^0 (J mol ⁻¹ K ⁻¹)	-37.28	$\Delta S^{0\tau}$ (J mol ⁻¹ K ⁻¹)	-37.28
		ΔG^0 (KJ mol ⁻¹)	-18.47	$\Delta G^{0\tau}$ (KJ mol ⁻¹)	-18.47

Mean errors in variables are as follows: $\Delta H^0 = \pm 0.01$ kJ mol⁻¹; $\Delta S^0 = \pm 0.01$ J mol⁻¹K⁻¹; $\Delta G^{0\tau} = \pm 0.01$ kJ mol⁻¹; $\Delta H^{0\tau} = \pm 0.01$ kJ mol⁻¹; $\Delta S^{0\tau} = \pm 0.01$ J mol⁻¹K⁻¹

Table 3. Association constants (K_a^Φ) and standard free energy changes for (HSA +THC), (HSA+THC+ α -CD) and (HSA+THC+ β -CD) systems at 298.15 K.

System	HSA+THC	HSA+THC+ α -CD	HSA+THC+ β -CD
$K_a^\Phi \times 10^3$ (M ⁻¹)	4.21	3.03	2.49
$\Delta G^{\Phi 0}$ (KJ mol ⁻¹)	-20.24	-19.44	-18.97

Table S1. UV-Vis spectroscopic data for the generation of Job plots of aqueous THC+ α -CD system at 298.15 K^a and 236 nm.

THC + ALPHA – CYCLODEXTRIN							
THC (mL)	α -CD (mL)	THC (μ M)	α -CD (μ M)	$\frac{[\text{THC}]}{[\text{THC}] + [\alpha - \text{CD}]}$	Absorbance (A)	ΔA	$\frac{\Delta A \times [\text{THC}]}{[\text{THC}] + [\alpha - \text{CD}]}$
0	3	0	100	0	0.0000	1.1139	0.0000
0.3	2.7	10	90	0.1	0.1360	0.9779	0.0978
0.6	2.4	20	80	0.2	0.2421	0.8718	0.1744
0.9	2.1	30	70	0.3	0.3396	0.7743	0.2323
1.2	1.8	40	60	0.4	0.4380	0.6759	0.2703
1.5	1.5	50	50	0.5	0.5460	0.5679	0.2839
1.8	1.2	60	40	0.6	0.6365	0.4774	0.2864
2.1	0.9	70	30	0.7	0.7857	0.3281	0.2297
2.4	0.6	80	20	0.8	0.9233	0.1905	0.1524
2.7	0.3	90	10	0.9	1.0359	0.0780	0.0702
3	0	100	0	1	1.1139	0.0000	0.0000

^aStandard uncertainties in temperature u are: $u(T) = \pm 0.01$ K.

Table S2. UV-Vis spectroscopic data for the generation of Job plots of aqueous THC+ α -CD system at 298.15 K^a and 263 nm.

THC + ALPHA – CYCLODEXTRIN							
THC (mL)	α -CD (mL)	THC (μ M)	α -CD (μ M)	$\frac{[\text{THC}]}{[\text{THC}] + [\alpha - \text{CD}]}$	Absorbance (A)	ΔA	$\frac{\Delta A \times [\text{THC}]}{[\text{THC}] + [\alpha - \text{CD}]}$
0	3	0	100	0	0.0000	1.0006	0.0000
0.3	2.7	10	90	0.1	0.1069	0.8937	0.0894
0.6	2.4	20	80	0.2	0.1901	0.8105	0.1621
0.9	2.1	30	70	0.3	0.2736	0.7270	0.2181
1.2	1.8	40	60	0.4	0.3602	0.6404	0.2562
1.5	1.5	50	50	0.5	0.4603	0.5403	0.2701
1.8	1.2	60	40	0.6	0.5545	0.4461	0.2677
2.1	0.9	70	30	0.7	0.6906	0.3100	0.2170
2.4	0.6	80	20	0.8	0.8073	0.1933	0.1547
2.7	0.3	90	10	0.9	0.9063	0.0943	0.0849
3	0	100	0	1	1.0006	0.0000	0.0000

Table S3. UV-Vis spectroscopic data for the generation of Job plots of aqueous THC+ β -CD system at 298.15 K^a and 236 nm.

THC+BETA – CYCLODEXTRIN							
THC (mL)	β -CD (mL)	THC (μ M)	β -CD (μ M)	$\frac{[\text{THC}]}{[\text{THC}] + [\beta - \text{CD}]}$	Absorbance (A)	ΔA	$\frac{\Delta A \times [\text{THC}]}{[\text{THC}] + [\beta - \text{CD}]}$
0	3	0	100	0	0.0000	1.0698	0.0000
0.3	2.7	10	90	0.1	0.1188	0.9510	0.0951
0.6	2.4	20	80	0.2	0.2082	0.8616	0.1723
0.9	2.1	30	70	0.3	0.3368	0.7330	0.2199
1.2	1.8	40	60	0.4	0.4364	0.6334	0.2534
1.5	1.5	50	50	0.5	0.5505	0.5192	0.2596
1.8	1.2	60	40	0.6	0.6621	0.4077	0.2446
2.1	0.9	70	30	0.7	0.7480	0.3217	0.2252
2.4	0.6	80	20	0.8	0.8576	0.2122	0.1698
2.7	0.3	90	10	0.9	0.9648	0.1049	0.0944
3	0	100	0	1	1.0698	0.0000	0.0000

Table S4. UV-Vis spectroscopic data for the generation of Job plots of aqueous THC+ β -CD system at 298.15 K^a and 263 nm.

THC+ BETA - CYCLODEXTRIN							
THC (mL)	β -CD (mL)	THC (μ M)	β -CD (μ M)	$\frac{[\text{THC}]}{[\text{THC}] + [\beta - \text{CD}]}$	Absorbance (A)	ΔA	$\frac{\Delta A \times [\text{THC}]}{[\text{THC}] + [\beta - \text{CD}]}$
0	3	0	100	0	0.0000	0.9661	0.0000
0.3	2.7	10	90	0.1	0.0913	0.8748	0.0875
0.6	2.4	20	80	0.2	0.1621	0.8040	0.1608
0.9	2.1	30	70	0.3	0.2759	0.6902	0.2071
1.2	1.8	40	60	0.4	0.3559	0.6103	0.2441
1.5	1.5	50	50	0.5	0.4633	0.5028	0.2514
1.8	1.2	60	40	0.6	0.5568	0.4093	0.2456
2.1	0.9	70	30	0.7	0.6437	0.3224	0.2257
2.4	0.6	80	20	0.8	0.7421	0.2240	0.1792
2.7	0.3	90	10	0.9	0.8463	0.1198	0.1078
3	0	100	0	1	0.9661	0.0000	0.0000

^aStandard uncertainties in temperature u are: $u(T) = \pm 0.01$ K.

Table S5. UV-vis spectroscopic data for the Benesi-Hildebrand double reciprocal plot of (THC+ α -CD) system at 298.15 to 308.15 K^a and 236 nm.

Temp (K ^a)	THC (μ M)	α -CD (μ M)	A _o	A	Δ A	1/[α -CD] (M ⁻¹)	1/ Δ A	Intercept	Slope	K _a (M ⁻¹ \times 10 ⁻³)
298.15	50	30	0.4994	0.5337	0.0343	0.0333	29.1698	1.0717	839.4	1.28
	50	40		0.5455	0.0461	0.0250	21.6693			
	50	50		0.5541	0.0547	0.0200	18.2715			
	50	60		0.5666	0.0672	0.0167	14.8702			
	50	70		0.5757	0.0763	0.0143	13.1116			
303.15	50	30	0.4986	0.5326	0.0340	0.0333	29.4273	0.966	859.1	1.12
	50	40		0.5426	0.0440	0.0250	22.7024			
	50	50		0.5527	0.0541	0.0200	18.4740			
	50	60		0.5664	0.0678	0.0167	14.7387			
	50	70		0.5734	0.0748	0.0143	13.3747			
308.15	50	30	0.4977	0.5314	0.0336	0.0333	29.7191	0.7515	873.27	0.86
	50	40		0.5417	0.0440	0.0250	22.7197			
	50	50		0.5512	0.0535	0.0200	18.6928			
	50	60		0.5658	0.0681	0.0167	14.6811			
	50	70		0.5725	0.0747	0.0143	13.3807			

Table S6. UV-vis spectroscopic data for the Benesi-Hildebrand double reciprocal plot of (THC+ α -CD) system at 298.15 to 308.15 K^a and 263 nm.

Temp (K ^a)	THC (μ M)	α -CD (μ M)	A ₀	A	ΔA	1/[α -CD] (M ⁻¹)	1/ ΔA	Intercept	Slope	K _a (M ⁻¹ $\times 10^{-3}$)
298.15	50	30	0.4138	0.4422	0.0284	0.0333	35.2033	1.1361	1011.9	1.12
	50	40		0.4542	0.0404	0.0250	24.7547			
	50	50		0.4559	0.0421	0.0200	23.7804			
	50	60		0.4723	0.0585	0.0167	17.0961			
	50	70		0.4786	0.0648	0.0143	15.4353			
303.15	50	30	0.4357	0.4616	0.0258	0.0333	38.7174	0.9986	1168.8	0.85
	50	40		0.4667	0.0310	0.0250	32.2933			
	50	50		0.4756	0.0398	0.0200	25.1165			
	50	60		0.4875	0.0518	0.0167	19.3059			
	50	70		0.4936	0.0578	0.0143	17.2966			
308.15	50	30	0.4254	0.4505	0.0252	0.0333	39.7079	0.7447	1192.2	0.62
	50	40		0.4584	0.0330	0.0250	30.2706			
	50	50		0.4604	0.0351	0.0200	28.5016			
	50	60		0.4789	0.0535	0.0167	18.6870			
	50	70		0.4847	0.0594	0.0143	16.8451			

Table S7. UV-vis spectroscopic data for the Benesi-Hildebrand double reciprocal plot of (THC+ β -CD) system at 298.15 to 308.15 K^a and 236 nm.

Temp (K ^a)	THC (μ M)	α -CD (μ M)	A ₀	A	ΔA	1/[α -CD] (M ⁻¹)	1/ ΔA	Intercept	Slope	K _a (M ⁻¹ $\times 10^{-3}$)
298.15	50	30	0.4994	0.5351	0.0357	0.0333	28.0253	1.5026	792.53	1.90
	50	40		0.5471	0.0477	0.0250	20.9432			
	50	50		0.5559	0.0565	0.0200	17.6897			
	50	60		0.5672	0.0678	0.0167	14.7387			
	50	70		0.5780	0.0786	0.0143	12.7278			
303.15	50	30	0.4986	0.5342	0.0356	0.0333	28.1041	1.3224	815.43	1.62
	50	40		0.5432	0.0446	0.0250	22.3973			
	50	50		0.5543	0.0557	0.0200	17.9436			
	50	60		0.5687	0.0701	0.0167	14.2555			
	50	70		0.5754	0.0768	0.0143	13.0262			
308.15	50	30	0.4977	0.5329	0.0351	0.0333	28.4508	1.0958	824.43	1.33
	50	40		0.5436	0.0459	0.0250	21.7795			
	50	50		0.5527	0.0550	0.0200	18.1830			
	50	60		0.5687	0.0710	0.0167	14.0816			
	50	70		0.5742	0.0764	0.0143	13.0831			

Table S8. UV-vis spectroscopic data for the Benesi-Hildebrand double reciprocal plot of (THC+ β -CD) system at 298.15 to 308.15 K^a and 263 nm.

Temp (K ^a)	THC (μ M)	α -CD (μ M)	A ₀	A	Δ A	1/[α -CD] (M ⁻¹)	1/ Δ A	Intercept	Slope	K _a (M ⁻¹ $\times 10^{-3}$)
298.15	50	30	0.4138	0.4547	0.0409	0.0333	24.4383	1.1691	698.68	1.67
	50	40		0.4684	0.0546	0.0250	18.3205			
	50	50		0.4772	0.0634	0.0200	15.7846			
	50	60		0.4916	0.0778	0.0167	12.8543			
	50	70		0.5064	0.0926	0.0143	10.8034			
303.15	50	30	0.4357	0.4691	0.0334	0.0333	29.9619	1.2649	845.09	1.50
	50	40		0.4833	0.0475	0.0250	21.0437			
	50	50		0.4876	0.0519	0.0200	19.2762			
	50	60		0.5045	0.0688	0.0167	14.5341			
	50	70		0.5079	0.0721	0.0143	13.8643			
308.15	50	30	0.4254	0.4469	0.0215	0.0333	46.4261	1.5487	1364.6	1.13
	50	40		0.4532	0.0279	0.0250	35.8995			
	50	50		0.4577	0.0324	0.0200	30.8866			
	50	60		0.4685	0.0431	0.0167	23.1797			
	50	70		0.4742	0.0488	0.0143	20.4792			

Table S9. Data of the van't Hoff equation for calculation of thermodynamic parameters ΔH^0 , ΔS^0 and ΔG^0 of different (THC+ α -CD) inclusion complexes at $\lambda_{\max} = 236$ and 263 nm.

λ_{\max} (nm)	T (K ^a)	1/T	Ka (M ⁻¹ ×10 ⁻³)	lnKa	Slope	Intercept	ΔH^0 (KJ mol ⁻¹)	ΔS^0 (J mol ⁻¹ K ⁻¹)	ΔG^0 (KJ mol ⁻¹)
236	298.15	0.00335	1.28	7.1521	3,616.90	-4.9551	-30.07	-41.20	-17.79
	303.15	0.00330	1.12	7.0250					
	308.15	0.00325	0.86	6.7576					
263	298.15	0.00335	1.12	7.0235	5,384.50	-11.028	-44.77	-91.69	-17.43
	303.15	0.00330	0.85	6.7504					
	308.15	0.00325	0.62	6.4372					

Table S10. Data of the van't Hoff equation for calculation of thermodynamic parameters ΔH^0 , ΔS^0 and ΔG^0 of different (THC+ β -CD) inclusion complexes at $\lambda_{\max} = 236$ and 263 nm.

λ_{\max} (nm)	T (K ^a)	1/T	Ka (M ⁻¹ ×10 ⁻³)	lnKa	Slope	Intercept	ΔH^0 (KJ mol ⁻¹)	ΔS^0 (J mol ⁻¹ K ⁻¹)	ΔG^0 (KJ mol ⁻¹)
236	298.15	0.00335	1.90	7.5475	3,260.70	-3.381	-27.11	-28.11	-18.73
	303.15	0.00330	1.62	7.3912					
	308.15	0.00325	1.33	7.1923					
263	298.15	0.00335	1.67	7.4226	3,558.30	-4.4839	-29.59	-37.28	-18.47
	303.15	0.00330	1.50	7.3111					
	308.15	0.00325	1.13	7.0343					

Table S11. Data of the van't Hoff equation for calculation of thermodynamic parameters $\Delta H^{\tau 0}$, $\Delta S^{\tau 0}$ and $\Delta G^{\tau 0}$ of different (THC+ α -CD) inclusion complexes at $\lambda_{\max} = 236$ and 263 nm.

λ_{\max} (nm)	T (K ^a)	1/T	K_a^{τ} (M ⁻¹ ×10 ⁻³)	ln K_a^{τ}	Slope	Intercept	$\Delta H^{\tau 0}$ (KJ mol ⁻¹)	$\Delta S^{\tau 0}$ (J mol ⁻¹ K ⁻¹)	$\Delta G^{\tau 0}$ (KJ mol ⁻¹)
236	298.15	0.00335	1.30	7.1676	3,646.30	-5.0485	-30.32	-41.98	-17.80
	303.15	0.00330	1.10	7.0071					
	308.15	0.00325	0.87	6.7703					
263	298.15	0.00335	1.22	7.1088	5,889.60	-12.671	-48.97	-105.35	-17.56
	303.15	0.00330	0.81	6.7024					
	308.15	0.00325	0.64	6.4687					

Table S12. Data of the van't Hoff equation for calculation of thermodynamic parameters $\Delta H^{\tau 0}$, $\Delta S^{\tau 0}$ and $\Delta G^{\tau 0}$ of different (THC+ β -CD) inclusion complexes at $\lambda_{\max} = 236$ and 263 nm.

λ_{\max} (nm)	T (K ^a)	1/T	K_a^{τ} (M ⁻¹ ×10 ⁻³)	ln K_a^{τ}	Slope	Intercept	$\Delta H^{\tau 0}$ (KJ mol ⁻¹)	$\Delta S^{\tau 0}$ (J mol ⁻¹ K ⁻¹)	$\Delta G^{\tau 0}$ (KJ mol ⁻¹)
236	298.15	0.00335	2.10	7.6478	4,908.10	-8.8301	-40.81	-73.42	-18.92
	303.15	0.00330	1.52	7.3276					
	308.15	0.00325	1.23	7.1141					
263	298.15	0.00335	1.47	7.2953	3,558.30	-4.4839	-29.59	-37.28	-18.47
	303.15	0.00330	1.20	7.0874					
	308.15	0.00325	0.93	6.8405					

Table S13. ^1H NMR data of the pure thiamine hydrochloride, pure α -Cyclodextrin, β -Cyclodextrin and the respective inclusion complexes.

α -Cyclodextrin (400 MHz, Solvent: D_2O), δ/ppm	β -Cyclodextrin (400 MHz, Solvent: D_2O), δ/ppm
3.161-3.207 (6H, t, J = 18.400 Hz), 3.217-3.250 (6H, dd, J = 5.200, 13.200 Hz), 3.436-3.562 (18H, m), 3.585-3.609 (6H, t, J = 9.600 Hz), 4.659-4.650 (6H, d, J = 3.600 Hz)	3.399-3.444 (7H, t, J = 18.000 Hz), 3.472-3.506 (7H, dd, J = 6.400 Hz, 13.6 Hz), 3.692-3.751 (21H, m), 3.776-3.823 (7H, t, J = 18.800 Hz), 4.904-4.913 (7H, d, J = 3.600 Hz)
Thiamine hydrochloride (400 MHz, Solvent: D_2O), δ/ppm	
2.386(3H, s), 2.472(3H, s), 3.018-3.047(2H, t, J=5.600Hz), 3.710-3.739(2H, t, J=6.00Hz), 5.412(2H, s), 7.868(1H, s), 9.509(1H, s)	
THC+ α -CD inclusion complex (400 MHz, Solvent: D_2O), δ/ppm	THC+ β -CD inclusion complex (400 MHz, Solvent: D_2O), δ/ppm
2.406(3H, s), 2.493(3H,s), 3.055-3.082(2H, t, J=5.4), 3.451-3.513(14H, m), 3.707-3.870(24H,m), 4.922-4.932(6H, d, J=4.0), 5.430(2H, s),7.876(1H, s), 9.523(1H, s)	2.444(3H, s), 2.531(3H, s),3.075-3.105(2H, t, J=6.000Hz),3.486-3.567(16H, m), 3.780-3.883(28H, m), 4.976-4.996(7H,d, J=8Hz), 5.467(2H, s),7.917(1H, s),9.550(1H,s)

Table S14. Frequencies of FTIR spectra of α -CD, β -CD, THC and two solid inclusion complexes

α -cyclodextrin (α -CD)		β -cyclodextrin (β -CD)	
Wavenumber (cm^{-1})	Group	Wavenumber (cm^{-1})	Group
3410.09	-O-H stretching	3424.05	-O-H stretching
2927.18	-C-H stretching	2927.31	-C-H stretching
1363.21	-C-H and -O-H bending	1398.37	-C-H and -O-H bending
1152.27	C-O-C bending	1160.32	C-O-C bending
1033.25	C-C-O stretching	1030.39	C-C-O stretching
950.32	skeletal vibration involving α -1,4linkage	940.29	skeletal vibration involving α -1,4linkage
Thiamine hydrochloride (THC)			
Wavenumber (cm^{-1})		Group	
3436.05		Broad band of merged spectra due to the presence of NH_2 and -OH stretching	
2361.26		-CH ₂ out of plane bending	
1636.35		Bend N-H (NH_2) stretching	
1000.03		Deformation N-H (NH_2)	
1614.02-1380.15		Pyrimidine ring stretching vibration	
1360.25		C-CH ₃ group	
1223.15		Stretching C-CH ₂ bridge of pyrimidine ring	
519.08		S-C-N and S-C-C out of plane deformation of thiazole ring	

(IC - 1) THC + α -CD		(IC - 2) THC + β -CD	
Wavenumber (cm ⁻¹)	Group	Wavenumber (cm ⁻¹)	Group
3420.09	-O-H stretching	3405.23	-O-H stretching
2914.19	-C-H stretching	2906.16	-C-H stretching
2365.21	-CH ₂ bending	2363.29	-CH ₂ bending
1632.02	C-O-C bending	1632.27	C-O-C bending
1153.25	Stretching C-CH ₂ bridge of pyrimidine ring	1157.33	Stretching C-CH ₂ bridge of pyrimidine ring
1029.13	C-C-O stretching	1027.11	C-C-O stretching

Table S15. Spectro-fluorimetric data for the Benesi-Hildebrand double reciprocal plot of (HSA+THC) system at 298.15 K^a.

HSA (g/L)	THC (μ M)	I_0	I	$I-I_0$	$1/[THC] (M^{-1})$	$1/\Delta I (\times 10^6)$	Intercept ($\times 10^7$)	Slope ($\times 10^{10}$)	$K_a^\phi (M^{-1} \times 10^{-3})$
0.1	20	3373138.75	3194777	178362.0	0.0500	5.6066	4.2954	1.0213	4.21
0.1	30		3101683	271455.5	0.0333	3.6838			
0.1	40		3034246	338893.3	0.0250	2.9508			
0.1	50		2987936	385202.8	0.0200	2.5960			
0.1	60		2901248	471891.3	0.0167	2.1191			

^aStandard uncertainties in temperature u are: $u(T) = \pm 0.01$ K.

Table S16. Spectro-fluorimetric data for the Benesi-Hildebrand double reciprocal plot of (HSA+THC) system in presence of fixed amount of α -CD at 298.15 K^a.

HSA (g/L)	THC (μ M)	I_0	I	$I-I_0$	$1/[\text{THC}]$ (M^{-1})	$1/\Delta I$ ($\times 10^6$)	Intercept ($\times 10^7$)	Slope ($\times 10^{10}$)	K_a^ϕ ($M^{-1} \times 10^{-3}$)
0.1	20	3373138.75	3201177	171962.0	0.0500	0.5815	3.3303	1.1004	3.03
0.1	30		3121683	251455.5	0.0333	0.3977			
0.1	40		3066246	306893.3	0.0250	0.3258			
0.1	50		2958936	414202.8	0.0200	0.2414			
0.1	60		2909248	463891.3	0.0167	0.2156			

Table S17. Spectro-fluorimetric data for the Benesi-Hildebrand double reciprocal plot of (HSA+THC) system in presence of fixed amount of β -CD at 298.15 K^a.

HSA (g/L)	THC (μ M)	I_0	I	$I-I_0$	$1/[\text{THC}]$ (M^{-1})	$1/\Delta I$ ($\times 10^6$)	Intercept ($\times 10^7$)	Slope ($\times 10^{10}$)	K_a^ϕ ($M^{-1} \times 10^{-3}$)
0.1	20	3373138.75	3211177	161962.0	0.0500	0.6174	2.9210	1.1743	2.49
0.1	30		3138683	234455.5	0.0333	0.4265			
0.1	40		3047246	325893.3	0.0250	0.3068			
0.1	50		2993936	379202.8	0.0200	0.2637			

0.1	60		2946248	426891.3	0.0167	0.2343			
-----	----	--	---------	----------	--------	--------	--	--	--

FIGURE

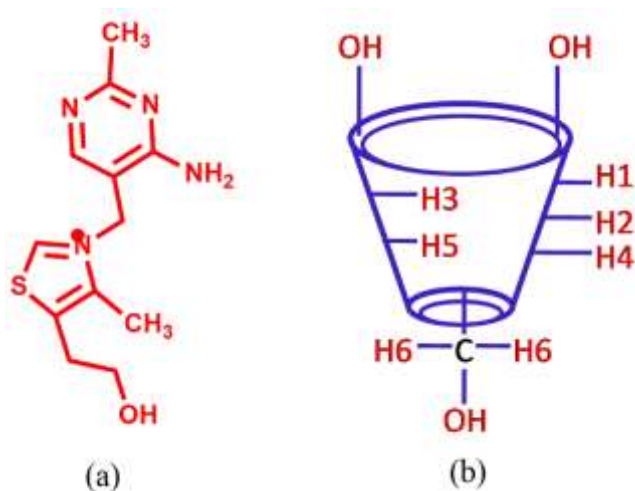


Figure 1: Molecular structures of (a) thiamine hydrochloride, (b) cyclodextrin

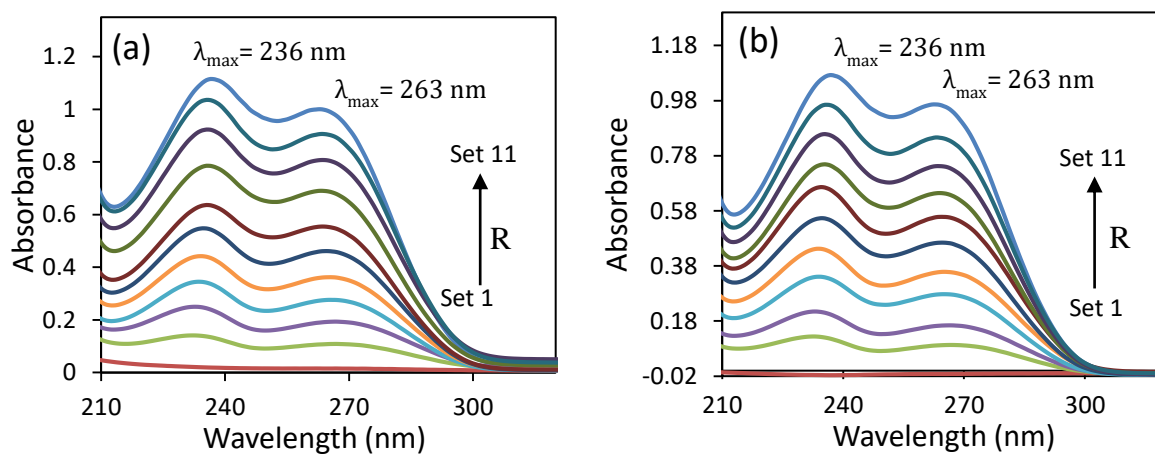


Figure 2(a,b): Spectra for the generation of Job plot of (a) THC+α-CD and (b) THC+β-CD systems at 236 and 263 nm.

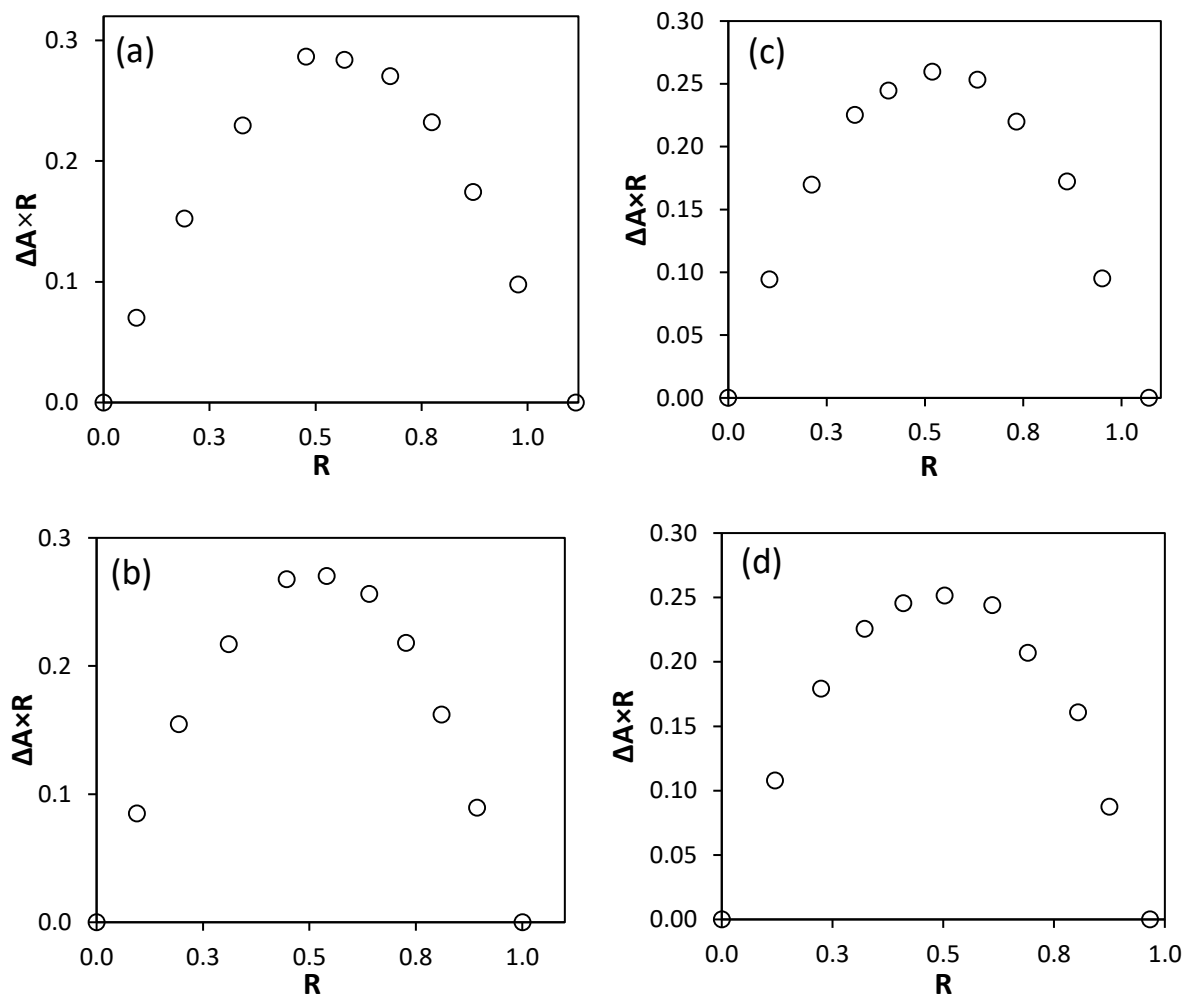


Figure 3(a,b,c,d): Job plots of the THC+ α -CD system at (a) $\lambda_{\max}=236$ nm, (b) $\lambda_{\max}=263$ nm and THC+ β -CD system at (c) $\lambda_{\max}=236$ nm, (d) $\lambda_{\max}=263$ nm

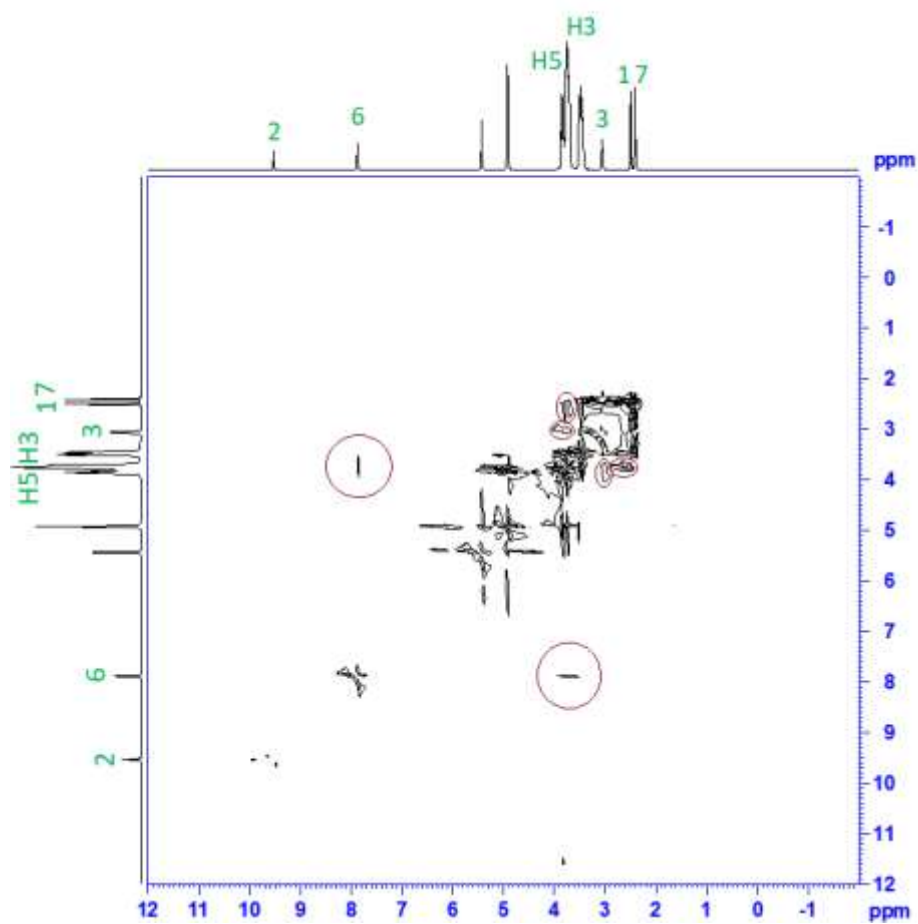


Figure 4. 2D ROESY NMR spectra of IC-1 (THC+α-CD)

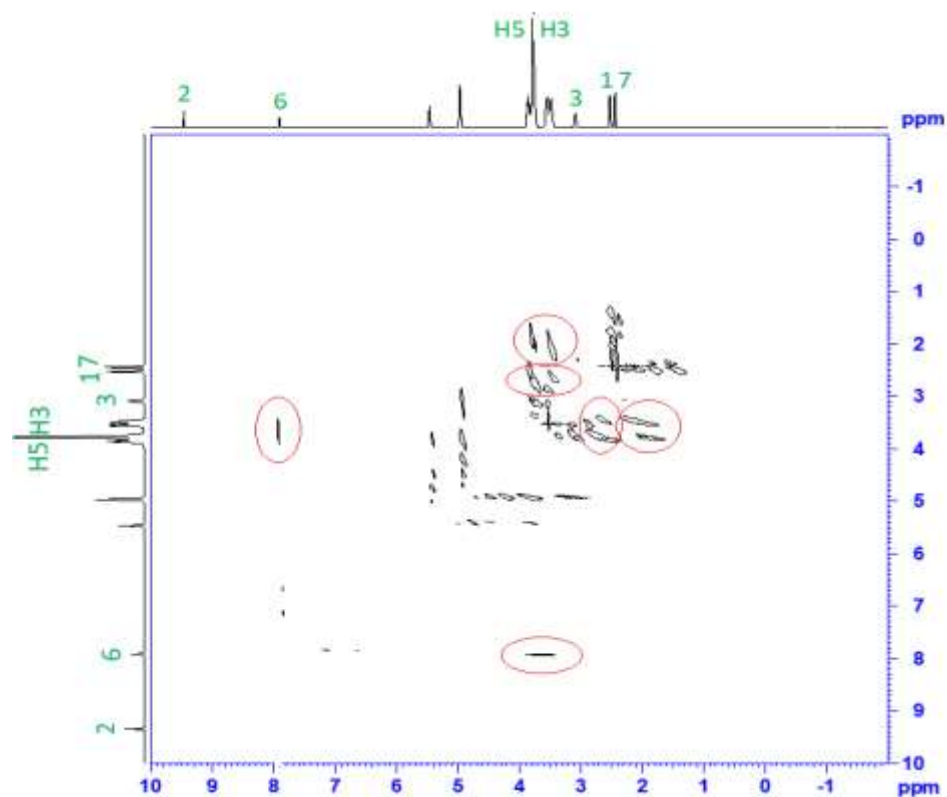


Figure 5. 2D ROESY NMR spectra of IC-2 (THC+ β -CD)

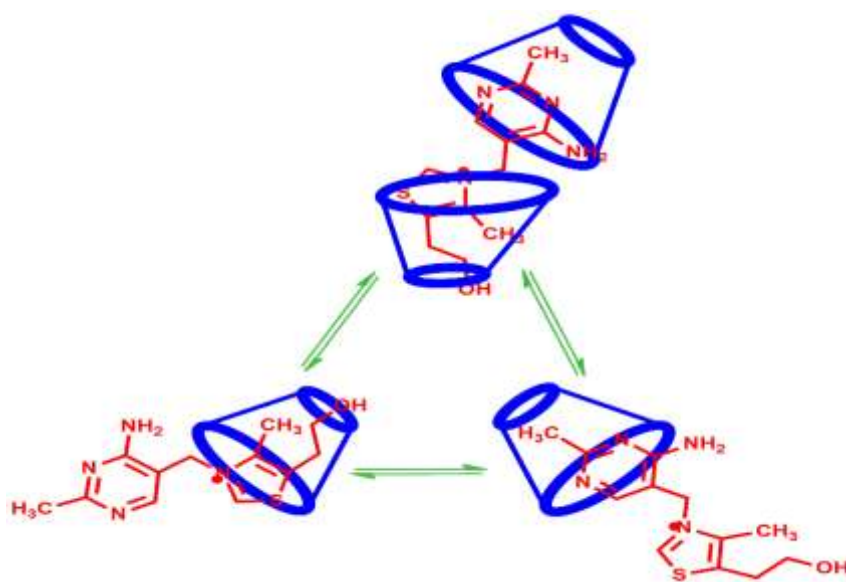


Figure 6: Plausible mechanism of inclusion complexation through wider rim of cyclodextrin.

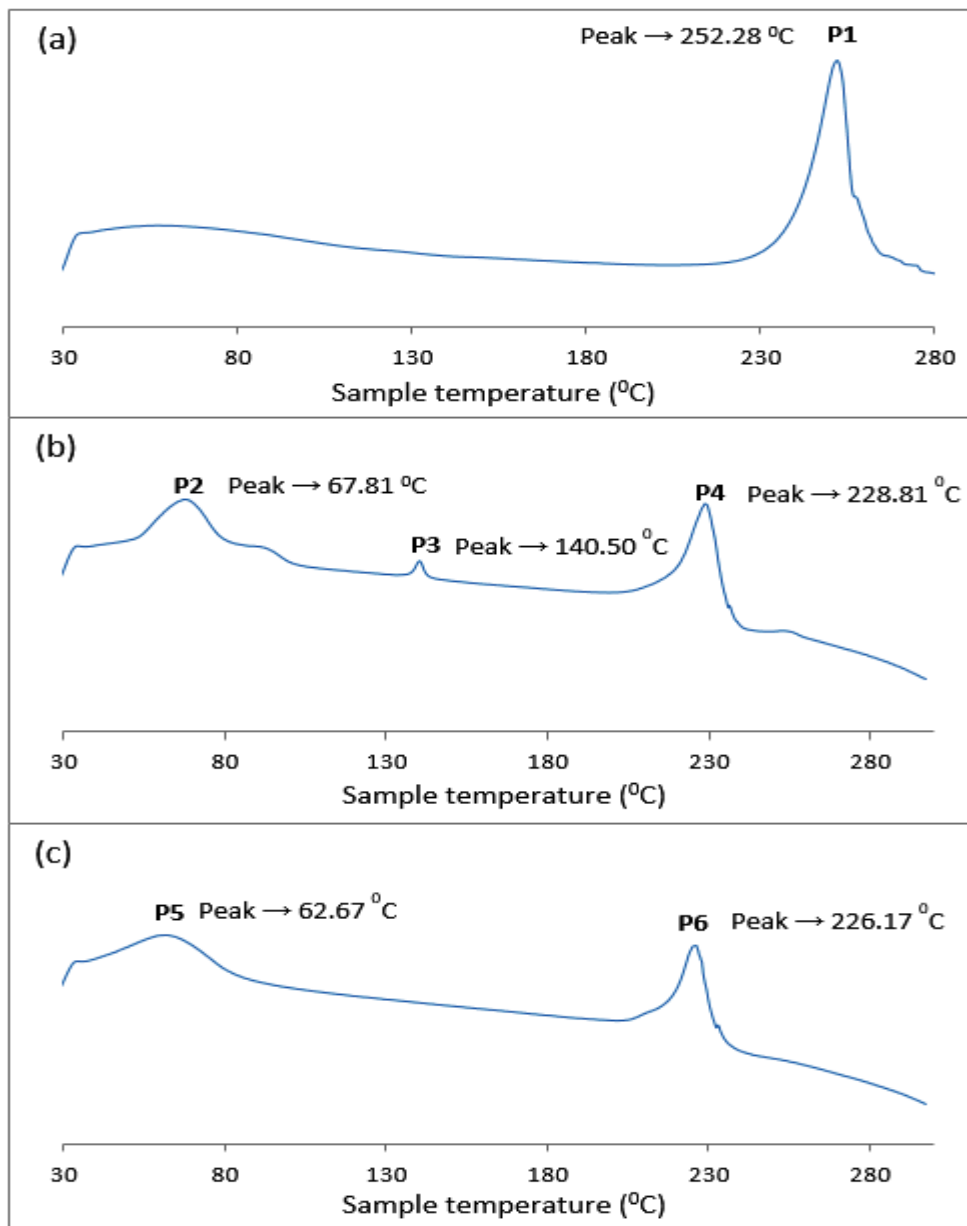


Figure 7(a,b,c):DSC thermogram of (a) THC, (b) THC+ α -CD, (c) THC+ β -CD

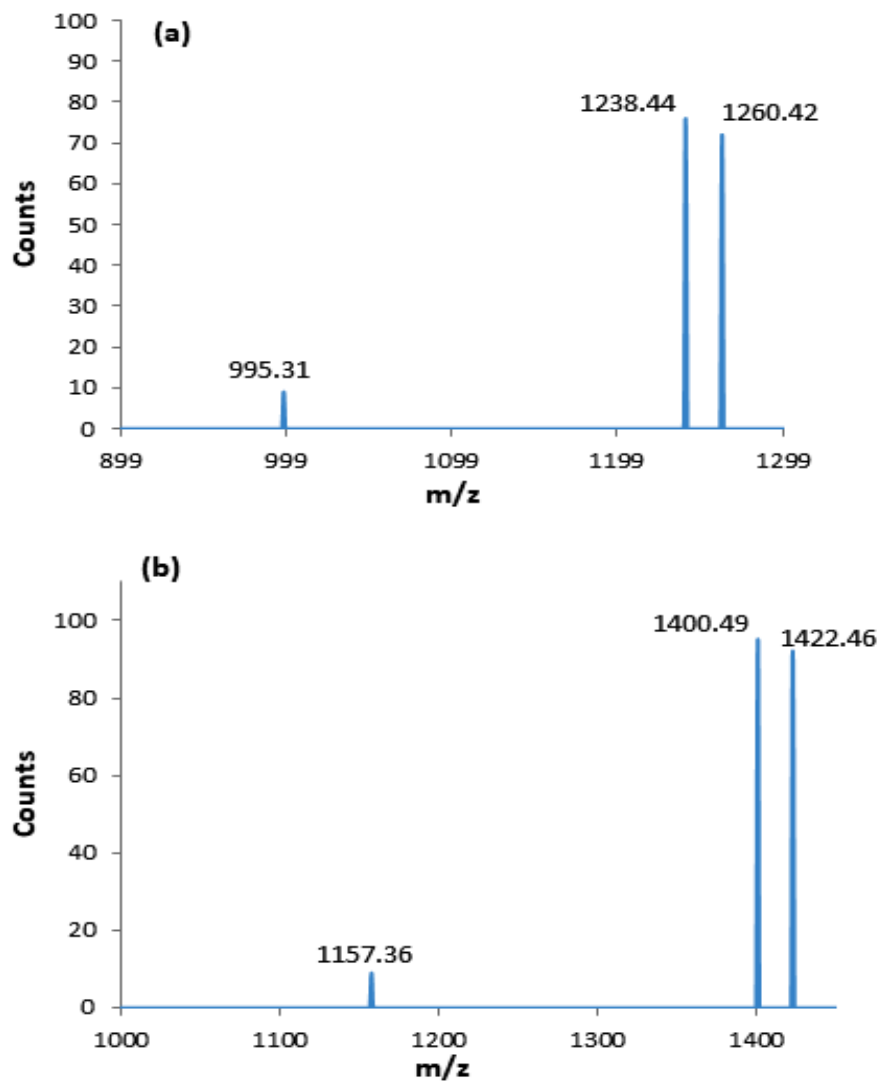


Figure 8(a,b): ESI- Mass spectra of (a) IC-1 (THC+ α -CD), (b) IC-2 (THC+ β -CD)

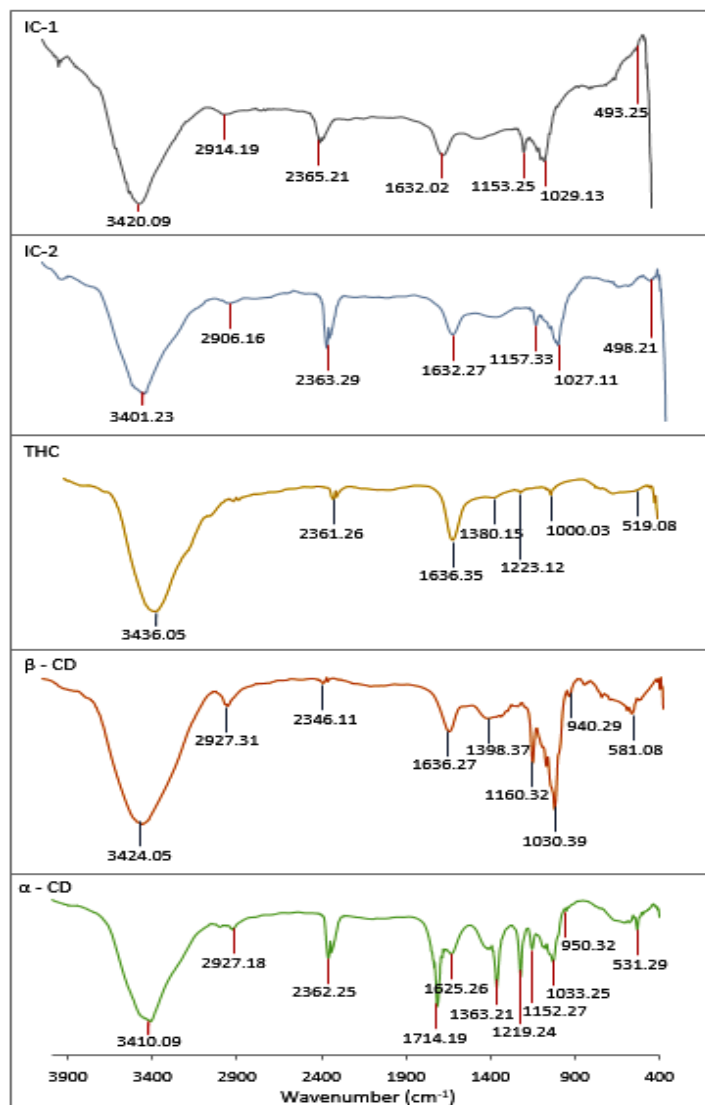


Figure 9(a,b,c):FTIR spectra of IC-1 (THC+ α -CD), IC-2(THC+ β -CD), THC, β -CD and α -CD

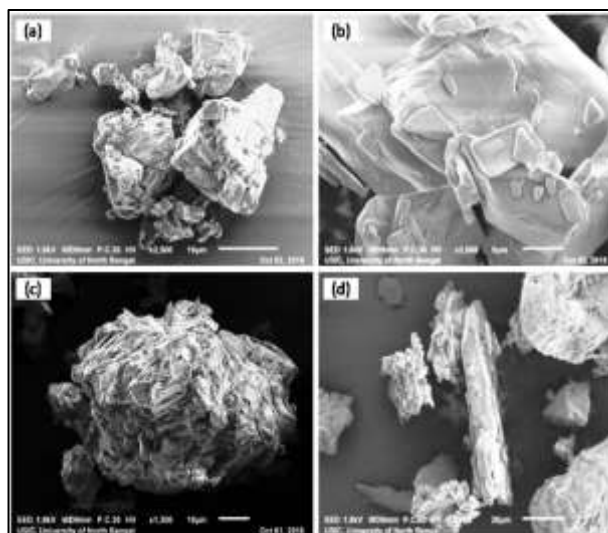


Figure 10(a,b,c,d):SEM images of (a) α -CD, (b) THC, (c) (THC+ α -CD) IC and (d) (THC+ α -CD) physical mixture.

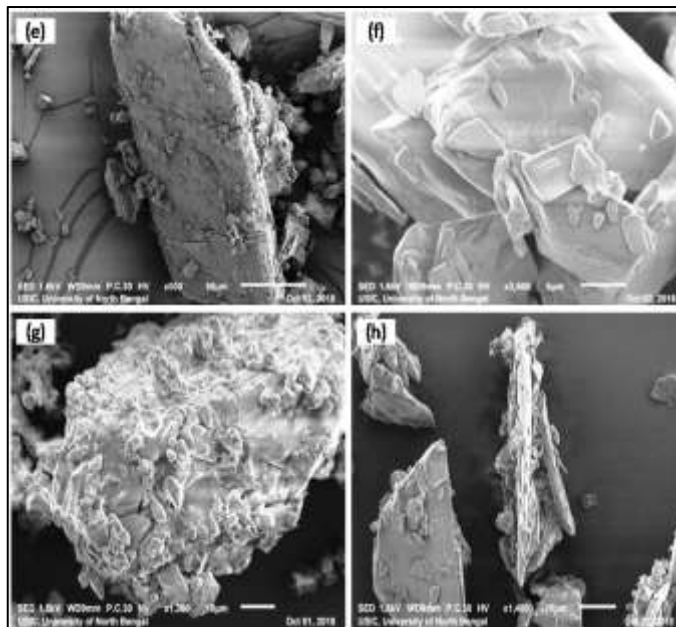
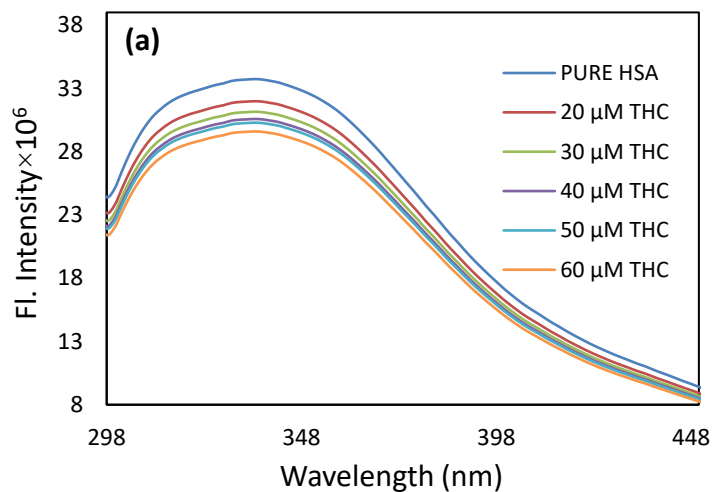


Figure 11(e,f,g,h):SEM images of (e) α -CD, (f) THC, (g) (THC+ α -CD) IC and (h) (THC+ α -CD) physical mixture.



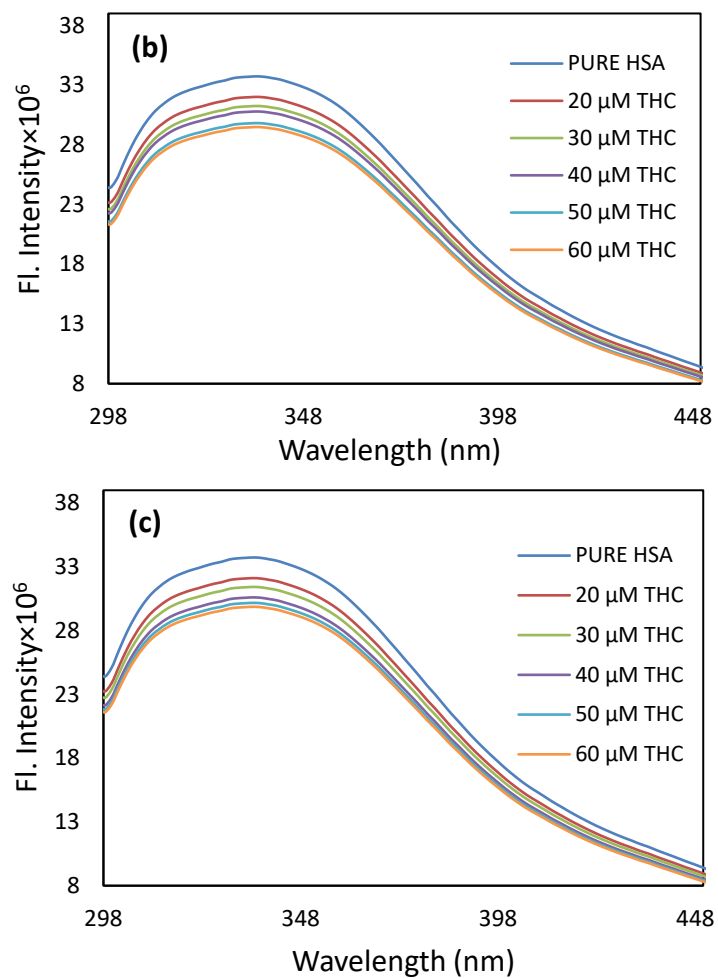


Figure 12(a, b, c): Fluorescence spectra of HSA molecule in presence of (a) THC, (b) THC along with β -CD (c) THC along with α -CD at the various concentrations.